DYNAMICS OF SECONDARY FLOW IN RECTANGULAR CHANNEL

Václav Uruba, Ondřej Hladík, Pavel Jonáš
Institute of Thermomechanics AS CR, v.v.i.

Abstract

Secondary flow in straight channel of rectangular cross-section is studied experimentally. Special attention is devoted to dynamics of secondary vortices in channel corner. The stereo time-resolved PIV method is used to acquire time series of the 3-component vector fields in plane perpendicular to the channel axis. The dynamics of the vortical structures is studied using Proper Orthogonal Decomposition method giving the energetic modes.

Introduction

After the initial observation by Nikuradse [13] the problem of secondary flows developing in ducts of a cross section with corners has attracted much attention. The problem has been studied from many points of view experimentally (see e.g. [4], [8], [9]), simulations of the Reynolds-averaged equations (see e.g. [5]), large eddy simulations (see e.g. [12]), and direct numerical simulations (e.g. [7]). The picture that emerges from these studies is that, from averaging over time and/or streamwise distance, a coherent motion of small amplitude exists, formed by eight vortices of very weak streamwise vorticity in the cross section, symmetric about the duct diagonals and the bisection lines.

Anyway, the large-scale secondary motions significantly alter the mean velocity contours in the cross section of the duct. Those structures are called secondary flow of 2nd kind. Such vortices differ from those usually observed near walls in turbulent boundary layers, because they are large-scale and are locked near the corners by the imposed geometric constraints. The observed structure is the cross-section aspect ratio dependent. Recent series of publications (see e.g. [2], [3], [6]) clarify some aspects of the secondary flow origin working on stability theory.

The longitudinal secondary vortices are considered to be stationary - see e.g. [9]. The references given above contain a lot of information on the steady mean structure of the secondary flow, however there is lack of information concerning the vortical structures dynamics. The presented paper is a contribution in this field.

Description of Experiment and Procedures

Our experiments have been carried out in the blow-down facility in the IT. The channel with cross-section 250 x 100 mm^2 and 3 meters in length has been used. Velocity of the air-flow was about 4.6 m/s in the channel inlet, top-hat profile with intensity of fluctuations less than 0.1 % and deviations of the mean velocity were less than 1 % throughout the cross-section.

The flow is subjected to experimental investigation in planes perpendicular to the mean flow. In the top-right corner area the 3-components of velocity are evaluated using the stereo-PIV. The coordinate system and area of interest is depicted in Fig. 1.

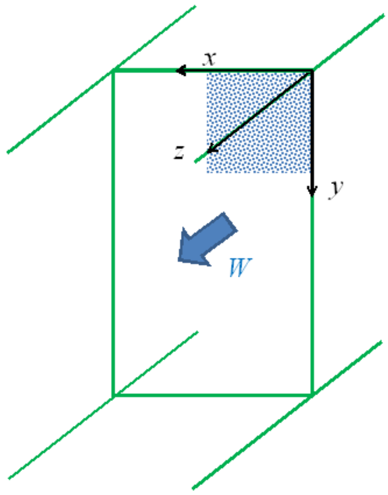

Fig. 1 – System of coordinates.

The stereo time-resolved PIV technique has been used to acquire data in the plane perpendicular to the channel axis. The DANTEC system consists of laser with cylindrical optics and 2 CMOS cameras and software Dynamics Studio 3.14. Laser New Wave Pegasus Nd:YLF, double head, wavelength 527 nm, maximal frequency 10 kHz, a shot energy is 10 mJ for 1 kHz (corresponding power 10 W per head). Cameras NanoSense MkIII, maximal resolution 1280 x 1024 pixels and corresponding maximal frequency 500 double-snaps per second. For particle generation the fog-generator SAFEX is used.

For analysis of the acquired dynamically changing velocity field we have used the Proper Orthogonal Decomposition (POD), identifying energetic structures in the flow-field – see [11]. The dynamics of the identified structures – modes are performed with help the POD modification Bi-Orthogonal Decomposition (BOD) defining both spatial modes (topos) and corresponding temporal modes (chronos). By truncation of low-energy modes we could study dynamics of the flow using low-dimensional dynamical system methods in phase space. The BOD method was proposed by Aubry et al. [1].

The proposed measurement procedure has been tested on the case of longitudinal vortical structures in the wake behind Ahmed body – see [14].

Results

The experiments were carried out in the *yz* plane in *x* distance 2.5 m from inlet. The 1600 doublesnaps with frequency 500 Hz were acquired forming the time series of 3.2 s.

First, the mean vector field was calculated and subtracted from all instantaneous pictures resulting in time series of fluctuations. In Fig. 2 the mean velocity distribution is shown, the in-plane velocity components *U* and *V* are represented by vectors, while the main-flow component *W* perpendicular to the measuring plane is shown as color. The coordinates are non-dimensioned using the channel width 100 mm.

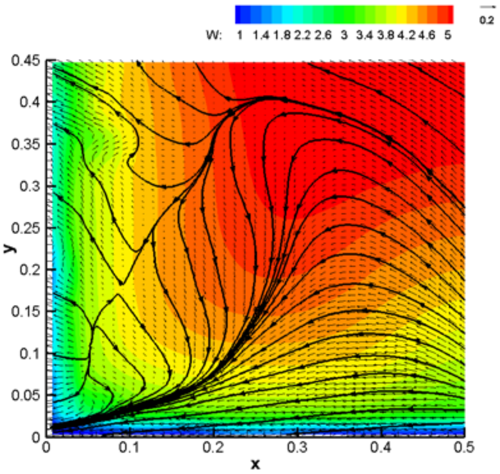

Fig. 2 – Mean velocity distribution

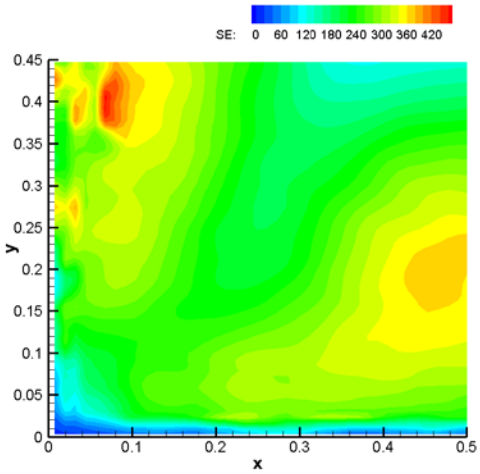

Fig. 3 – The total fluctuating energy

The mean flow structure corresponds to that described in literature as secondary structures of the 2nd kind.

In Fig. 3 the kinetic energy distribution in the cross-section is shown. The energy maxims are located in certain distance from the wall, while in the vicinity of the corner axis minimal fluctuating activity is detected. The small perturbation near wall for small *x* are connected with technical problems close to the wall (reflections).

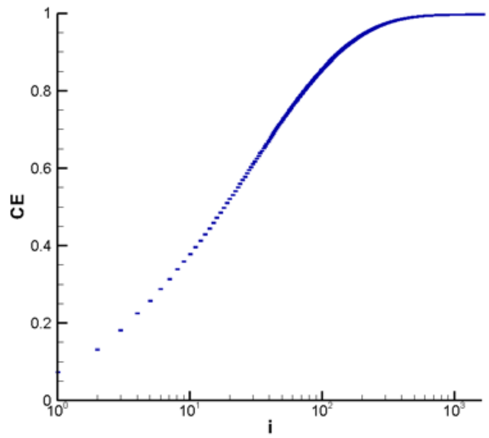

Fig. 4 – POD cumulative modes energy

The sequence of 1600 velocity fluctuations snapshots was subjected to standard POD analysis resulting into the same number of energetic modes ordered according to the kinetic energy content. In Fig. 4 the cumulative kinetic energy of the evaluated modes is shown. The first mode contains about 7.7 % of total fluctuating energy, while the first 5 modes in sum contain about 26 %, 10 modes 38 %, 50 modes 73 %, 100 modes 86 %, 200 modes 95 % and 400 modes almost 99 % of the total fluctuating kinetic energy.

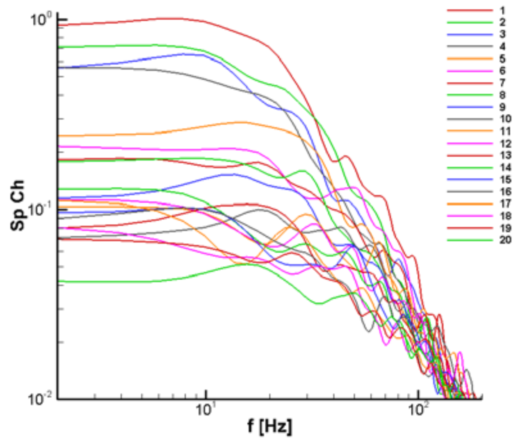

Fig. 5 – Spectra of first 20 chronoses

Generally, the low-order high-energy modes containing the most of kinetic energy related to the low-frequency dynamics. This was proved by analysis of corresponding chronoses. However the spectra of all chronoses are continuous of wide-band type with no distinct peaks on particular frequencies. In Fig. 5 the spectra of the first 20 chronoses are depicted. A few energy maxima could be detected. The first 3 modes have maximal energy on low frequencies between 5 and 10 Hz. The higher order modes exhibit considerably lower energy on those frequencies, however the high-frequency content (40 Hz and higher) is more or less the same.

Now a few toposes will be shown. In Fig. 6 the typical examples of toposes are presented. The color denoting *w* velocity component fluctuation is red for positive and blue for negative values. The typical dynamical structures could be recognized. Please note that the toposes are normalized to be orthonormal, however their energy differs (see Fig. 4). To see better the structures formed by vector field the vector lines are added.

The structures in energetic modes (toposes) are to be analyzed.

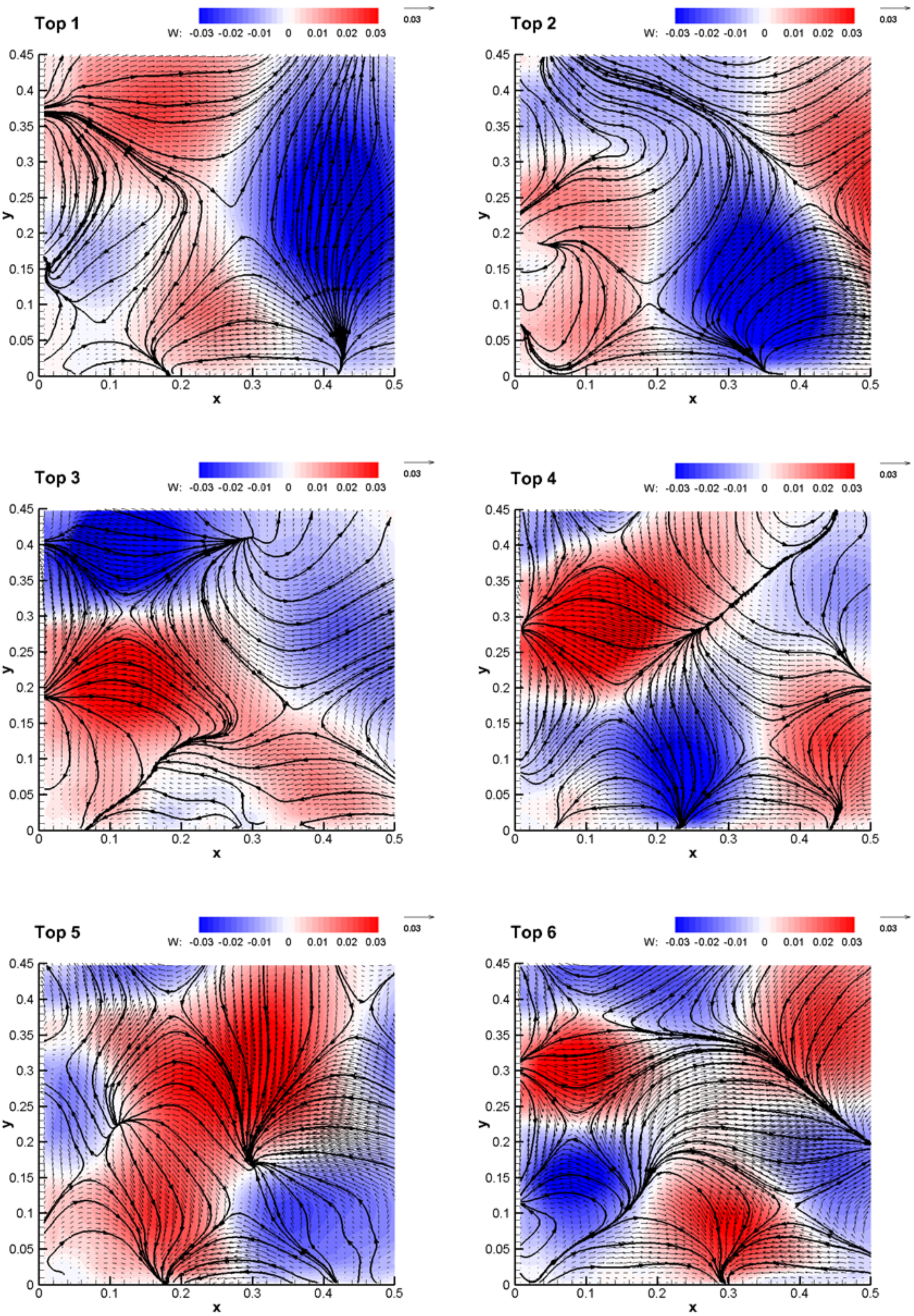
Top 1
Top 2
Top 3
Top 4
Top 5
Top 6
W: -0.03 -0.02 -0.01 0 0.01 0.02 0.03
0.03
x
y
0 0.1 0.2 0.3 0.4 0.5
0 0.05 0.1 0.15 0.2 0.25 0.3 0.35 0.4 0.45

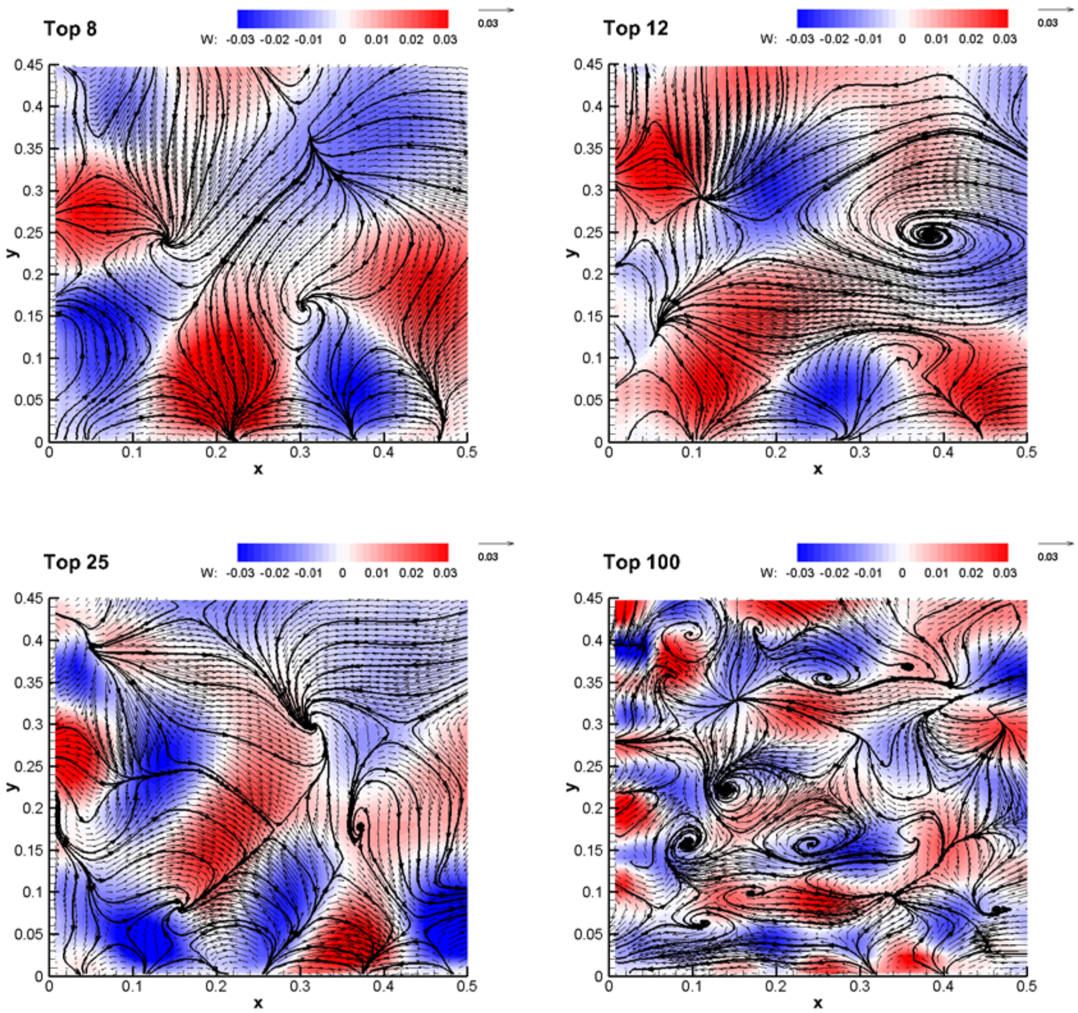

Fig. 6 – The Toposes Nos. 1, 2, 3, 5, 6, 12, 25 and 100

The velocity fluctuations in the mean-flow direction *w* form spots of pulsations, as the time modes (chronoses) represent positive and negative fluctuations with zero mean value.

The vector fields reveal the dynamic structures forming the secondary flows. We could recognize several types of structures, but surprisingly not many spirals corresponding to vortices. Typical structures for lower order modes are saddles, nodes and improper nodes forming curves as defined in [10]. The first vortical structure could be recognized in the 12^{th} topos – see Fig. 6.

The higher order mode, the smaller energy content and also the finer topological structures in correspondent topos. This effect is illustrated by the 100^{th} topos.

Conclusion

The dynamical structures in secondary flow of 2^{nd} kind in a channel of rectangular cross-section have been studied using stereo time-resolved PIV technique. The BOD method shows both time and space energetic modes. The 3 most energetic chronoses contain maximum energy for frequencies between 5 and 10 Hz. In toposes the pulsating spots of longitudinal velocity could be recognized. In-plane structures are typically saddles and nodes, while spirals (corresponding to vortices) are not very frequent.

Acknowledgement

The author gratefully acknowledges financial support of the Grant Agency of the Czech Republic, projects No. 101/08/1112 and P101/10/1230.

References

[1] Aubry, N., Guyonnet, R. & Lima, R. 1991 Spatiotemporal Analysis of Complex Signals: Theory and Applications. Journal of Statistical Physics, Nos.2/3, 64, 683-739.
[2] Biau, D., Soueid, H. & Bottaro, A. 2008 Transition to turbulence in duct ow. J. Fluid Mech., 596, 133-142.
[3] Bottaro, A., Soueid, H. & Galletti, B. 2006 Formation of Secondary Vortices in Turbulent Square-Duct Flow. AIAA JOURNAL, No. 4, 44, 803-811.
[4] Brundett, E. & Baines, W.D. 1964 The Production and Diff_usion of Vorticity in Duct Flow. J. Fluid Mech., 19, 375-394.
[5] Demuren, A.O. & Rodi, W. 1984 Calculation of Turbulence-Driven Secondary Motion in Non-Circular Ducts. J. Fluid Mech., 140, 189-222.
[6] Galletti, B. & Bottaro, A. 2004 Large-scale secondary structures in duct ow. J. Fluid Mech., 512, 85-94.
[7] Gavrilakis, S. 1992 Numerical Simulation of Low Reynolds-Number Turbulent Flow Through a Straight Square Duct. J. Fluid Mech., 244, 101-129.
[8] Gessner, F.B. 1973 The Origin of Secondary Flow in Turbulent Flow Along a Corner. J. Fluid Mech., 58, 1-25.
[9] Hoagland, L.C. 1960 Fully Developed Turbulent Flow in Straight Rectangular Ducts - Secondary Flow, Its Cause and Effect On The Primary Flow. PhD thesis, Massachusetts Institute of Technology.
[10] Kenwright, D. N. 1998 Automatic detection of open and closed separation and attachment lines. Proceedings of the conference on Visualization '98, Research Triangle Park, North Carolina, United States, 151-158.
[11] Lumley, J. L. 1967 The structure of inhomogeneous turbulent ows. In Atm.Turb. and Radio Wave Prop., (ed. Yaglom and Tatarsky eds.), pp.166-178, Nauka, Moskva.
[12] Madabhushi, R.K. & Vanka, S.P. 1991 Large Eddy Simulation of Turbulence-Driven Secondary Flow in a Square Duct. Physics of Fluids A, No. 11, 3, 2734-2745.
[13] Nikuradse, J. 1926 Untersuchungen uber die Geschwindigkeitsverteilung in Turbulenten Stromungen. Ph.D. Dissertation, Univ. of Gottingen, Gottingen, Germany.
[14] Uruba, V. 2010 Lateral Vortex Dynamics behind Ahmed body. Proceedings in Applied Mathematics and Mechanics, 10, 455-456.
[15] Uruba, V., Hladík, O. and Jonáš, P., Dynamics of secondary vortices in turbulent channel flow. In: 13 European Turbulence Conference, 12 - 15 September 2011, Warszaw, 6p.